HHS Public Access

Author manuscript

IEEE Trans Neural Syst Rehabil Eng. Author manuscript; available in PMC 2018 September 01.

Published in final edited form as:

IEEE Trans Neural Syst Rehabil Eng. 2017 September ; 25(9): 1375–1386. doi:10.1109/TNSRE.2016.2631446.

Enhanced control of cortical pyramidal neurons with micromagnetic stimulation

Seung Woo Lee and

Massachusetts General Hospital, Department of Neurosurgery, Harvard Medical School, MGH-Thier 415, 50 Blossom Street, Boston, MA 02114, USA

Shelley I. Fried

Boston VA Healthcare System, Rehabilitation, Research and Development, 150 South Huntington Avenue, Boston, MA 01230, and, Massachusetts General Hospital, Department of Neurosurgery, Harvard Medical School, MGH-Thier 415, 50 Blossom Street, Boston, MA 02114, USA

Abstract

Magnetic stimulation is less sensitive to the inflammatory reactions that plague conventional electrode-based cortical implants and therefore may be useful as a next-generation (implanted) cortical prosthetic. The fields arising from micro-coils are quite small however and thus, their ability to modulate cortical activity must first be established. Here, we show that layer V pyramidal neurons (PNs) can be strongly activated by micro-coil stimulation and further, the asymmetric fields arising from such coils do not simultaneously activate horizontally -oriented axon fibers, thus confining activation to a focal region around the coil. The spatially-narrow fields from micro-coils allowed the sensitivity of different regions within a single PN to be compared: while the proximal axon was most sensitive in naïve cells, repetitive stimulation over the apical dendrite led to a change in state of the neuron that reduced thresholds there to below those of the axon. Thus, our results raise the possibility that regardless of the mode of stimulation, penetration depths that target specific portions of the apical dendrite may actually be more effective than those that target Layer 6. Interestingly, the state change had similar properties to state changes described previously at the systems level, suggesting a possible neuronal mechanism underlying such responses.

Index Terms

Micro-magnetic stimulation (μMS); Cortical stimulation; Prefrontal cortex (PFC); Primary motor cortex (M1); Neural Prosthesis

I. Introduction

The ability of implanted electrodes to modulate the activity of cortical neurons has opened up the possibility of treatment for a wide range of neurological disorders. For example, the implantation of stimulating electrodes into primary visual cortex (V1) may allow vision to

Phone: (617) 726-3888, Fried.Shelley@mgh.harvard.edu.

be restored to the blind [1, 2]. In addition, stimulation of somatosensory cortex can restore sensations of touch and proprioception [3], e.g. for brain-computer interface (BCI) devices that strive to restore or replace limb function. Despite this potential and much ongoing effort however, several fundamental limitations associated with electric stimulation from implanted electrodes raise concerns about the long-term viability of this approach. For example, implantation into cortex induces a host of inflammatory responses; the resulting gliosis [3–8] can lead to encapsulation of the stimulating electrodes with a corresponding loss in effectiveness over time [3, 6]. Another limitation arises from the high sensitivity of axons of passage and other horizontally extending processes to electric stimulation – their inadvertent activation can greatly expand the spatial extent of the region influenced by stimulation and lead to a wide range of undesirable side effects [9, 10]. A third limitation is that the small surface areas of cortical electrodes coupled with relatively small charge density limits constrains the charge per phase that can be delivered before damage occurs to the electrode and/or the surrounding tissue. Importantly, damage may occur even at moderate amplitude levels, especially with chronic implants [11]. While careful adherence to charge density limitations may enhance performance stability, the other limitations have proven harder to overcome. Use of non-penetrating approaches, e.g. cortical surface electrodes, can alleviate some of these concerns but their use necessitates much stronger levels of stimulation and produces non-focal activation thereby limiting the effectiveness of such an approach [1, 6, 10].

Magnetic stimulation from micro-coils (μMS) has recently proven capable of modulating neural activity in both sensory [12] (non-cortical) and deep regions [13] of the brain. The potential use of such coils for implantation into cortex is intriguing because they have the potential to overcome many of the limitations described above. For example, the high permeability with which magnetic fields pass through biological tissue suggests that gliotic encapsulation (of an implanted coil) would not adversely affect the thresholds for activating nearby neurons. In addition, because magnetic activation does not require direct contact between metal electrode and neural tissue, the potential for adverse interactions is greatly reduced. A third potentially attractive feature of micro-coil implants arises from the spatially asymmetric electric fields that they induce: such fields can avoid the activation of passing axons [12, 13], a feature that would be of considerable benefit to applications in which focal activation is essential, e.g. the restoration of high-acuity vision [1, 2, 6, 9] or the targeting a specific region of the body in somatosensory cortex [3]. Asymmetric electric fields may even allow for selective activation of specific neuronal populations within a focal region of cortex. This too would be highly attractive as it might allow specific aspects of physiological signaling to be selectively restored.

The highly structured architecture of the cortex suggests that the depth at which stimulation is delivered will influence the resulting neuronal response. Layer 4 (L4), the input layer of cortex, is a potentially attractive target because its activation may lead to activation of the same cortical circuits that operate physiologically and therefore yield closer matches to physiological (natural) patterns. Alternatively, stimulation of L6 targets the highly-sensitive proximal axon of L5 pyramidal neurons (PNs), the primary output (projection) neurons of cortex, and could therefore be effective even without intact cortical circuits. Interestingly, previous studies that measured threshold vs. depth of penetration in V1 of non-human

primates (NHPs) have yielded conflicting results: in one case, electrodes inserted into L6 yielded the lowest thresholds [14] while in another study thresholds were lowest for a penetration depth corresponding to L4 [15]. Although methodological details may have contributed somewhat to the differences in the two studies [2], a better understanding of the relative sensitivity of individual layers is still needed especially since different depths of insertion may have other consequences as well. For example, stimulation of L3 in the rodent brain led to sparse and spatially diffuse responses [9], thought to arise from activation of the lateral fibers or axons that extend from neighboring neurons. The relative spread of activation arising from stimulation of other layers is not known and may be an important consideration in optimizing the depth of penetration. A systematic understanding of the factors that influence the response to stimulation should also include exploration of whether individual types of cortical neurons each have distinct responses to a given stimulus as has been shown for electric stimulation in other regions of the nervous system [16]. Response differences across cortical cell-types are especially important to understand because individual types can each project to different parts of the brain and are thus likely to subserve different functional roles [17]. Another important consideration is that the underlying state of the targeted region of the brain is known to significantly alter the sensitivity to stimulation [18, 19] but the cellular basis underlying state changes is not well understood.

Here, we measured the response of L5 PNs from the prefrontal (PFC) and primary motor (M1) cortices to stimulation from a micro-coil in the *in vitro* mouse brain slice. The small size of the coil relative to the length of these neurons allowed the induced fields to be confined to specific sub-regions of targeted cells and therefore the relative sensitivity of individual regions within a single neuron could be compared; measurements were made over both the proximal axon and the apical dendrite. In addition, the two main types of L5 PNs were studied separately so that sensitivity differences could be compared. Finally, we used prolonged repetitive stimulation to explore whether state-like changes could be induced in individual cells.

II. METHODS

A. Modeling of induced fields

Custom software, written in Matlab, was used to develop qualitative estimations of the electric fields (E-field) arising from the flow of current through a micro-coil. The modeled coil was highly similar to the coil used in previous physiological experiments and had a 0.5 × 0.5 mm square cross-section, 1 mm length and 21 turns (single layer).

From Faraday's Laws, the E-field, $\vec{E}$, is related to the time varying magnetic field by:

$$\nabla \times \vec{E} = -\frac{\partial \vec{B}}{\partial t} \quad (1)$$

Since the magnetic field, $\vec{B}$, can be obtained by taking the curl of the magnetic vector potential, $\vec{A}$, (i.e. $\vec{B} = \nabla \times \vec{A}$) the equation for E-field can be expressed as:

$$\vec{E} = -\frac{\partial \vec{A}}{\partial t} - \nabla \mathrm{V} \quad (2)$$

The scalar potential (∇V) arises from charge re-distribution at boundaries of different conductivity. To minimize the large redistribution that can occur at the boundary between air and cerebrospinal fluid (CSF), coils were submerged in the bath for all experiments. We ignored the smaller effect that arises at the boundary between CSF and gray matter (GM) [20] and since targeted neurons were generally parallel to the tissue surface they were less affected by the larger component of redistribution that occurs in the z direction (i.e. normal to surface). We also ignored the field intensification that occurs in GM due to the CSF-GM boundary as well as the boundary between white and gray matter which cause limited effects. While these simplifying assumptions will lead to some inaccuracies in our calculations, model use was restricted to only qualitative depictions of field distributions. Removal of the ∇V term results in:

$$\vec{E} = -\frac{\partial \vec{A}}{\partial t} \quad (3)$$

The magnetic vector potential is calculated from the coil geometry as follows:

$$\vec{A} = \frac{\mu_0 N i}{4\pi} \cdot \oint \frac{dl}{R} \quad (4)$$

(μ_0 : permeability constant; N: number of turns; i: electric current through the solenoid; R: vector between the coil segment and the target segment at which the E-field is calculated; dl: small segment of the coil)

Because the loop of the coil was square and the principal axis of the targeted pyramidal neuron (PN) was approximately parallel to one side of the coil (c.f. Fig. 1), the E-field along the PNs can be calculated by numerically integrating along the length of the coil loop.

$$\partial \vec{E}_x = -\frac{\mu_0 N \left(\frac{di}{dt}\right)}{4\pi} \cdot \frac{1}{R} dl_x \quad (5)$$

where the x-dimension corresponds to the long axis of the PN.

Integrating the $\partial \vec{E}_x$ with respect to the x component of the line gives the following equation for $\vec{E}_x$.

$$\vec{E}_x = -\frac{\mu_0 N\left(\frac{di}{dt}\right)}{4\pi} \cdot \ln\left[x - x_0 + \sqrt{(x-x_0)^2 + (y-y_0)^2 + (z-z_0)^2}\right]\Big|_{x_{01}}^{x_{02}} \quad (6)$$

In the above equation, the coil element lies at (x_0, y_0, z_0) and the E-field is calculated at (x, y, z). The x_{01} and the x_{02} represent the positions of the lower and upper boundaries of the coil element in the x-axis. The spatial gradient, $\frac{\partial \vec{E}_x}{\partial x}$, is calculated by taking the derivative of the analytical solution for $\vec{E}_x$ from Equation (6). The input current to the coil, i, was a 50 kHz sinusoidal waveform with an amplitude of 10 A.

B. Preparation and testing of micro-coils

We purchased commercially-available multilayer inductors (ELJ-RFR10JFB, Panasonic Electronic Devices Corporation of America, Knoxville, TN) and soldered (15-mils 44-resin core SN63PB37) (Kester, Itasca, IL) copper wire leads to each end (34-AWG, polyurethane inner coat and nylon over coat) (Belden, Richmond, IN). Assembled coils were coated with 10 μm thick parylene-C coating (EIC Laboratories, Norwood, MA, USA) to eliminate the possibility that responses would be mediated by a leakage of current from the coil assembly into the slice preparation. After coating, the coil was placed on the tip of a custom made plastic tube 300 mm long and the distal ends were attached to the signal and ground leads of a BNC connector. The custom made tube was fabricated from a disposable plastic pipette (BD Falcon Serological Pipet; 5 ml in 1/10 ml; BD Biosciences, San Jose, CA) and cut to 300 mm in length. This allowed the coil assembly to be secured to the micromanipulator for accurate positioning near the mouse brain slice.

The IR illumination system of the microscope allowed the outer boundaries of the coil/coating to be visualized during *in vitro* experiments and therefore the coil could be accurately positioned in the x-y plane, e.g. relative to specific regions within the PFC or M1 areas. However, the coil was opaque to IR illumination and so it was necessary to perform preliminary measurements to determine the distance between the lower edge of the coil and the brain slice (z-direction). The bottom edge of the coated coil was determined relative to a focal point at or near the top surface of the assembly so that the height of the coil above the brain slice could be reasonably estimated. In this manner, the distance from the brain preparation to the closest edge of the coil (inside coating) could be reliably controlled and was set to 100 μm in all experiments.

Each micro-coil assembly was tested both before and after each experiment to ensure that there was no leakage of electrical current from the coil into the bath [12, 13]. Coils were submerged in physiological solution (0.9% NaCl) and the impedance between one of the coil terminals and an electrode immersed in the physiological solution was measured before and after each electrophysiological experiment. Impedances above 200 MΩ (measurement frequencies: DC~100 kHz) were considered indicative of adequate insulation. The high impedance ensured that direct electrical currents did not contribute to any of the observed neural activity. The coil was regularly inspected under the microscope for signs of damage

and its DC resistance and the impedance of insulation were monitored on an ongoing basis to further minimize the possibility of coil breakdown.

C. Micro-magnetic stimulation drive

The output of a function generator (AFG3021B, Tektronix Inc., Beaverton, OR) was connected to a 1,000 W audio amplifier (PB717X, Pyramid Inc., Brooklyn, NY) with a gain of 2.87 V/V and a bandwidth of 70 kHz. The audio amplifier was powered by a battery (LC-R1233P, Panasonic Corp., Newark, NJ), thereby uncoupling the stimulation and recording systems. The output of the amplifier (input to the coil, see Figure 2a) was monitored with an oscilloscope (TDS2014C, Tektronix Inc., Beaverton, OR). Pulsatile stimuli from the function generator had amplitudes ranging from 0–10 V in steps of 0.5 V; the duration was 20 μs. The rate of increase of the leading edge was 18 ns/V; the decrease of the trailing edge was identical [13]. The output of the amplifier consisted of a sharp peak followed by a damped cosine waveform. The amplitude of the sharp peak ranged from 0–28.7 V and the slopes of the leading and trailing edges were 80 ns/V and its duration was ~20 μsec. The amplitude of the damped sinusoid was considerably smaller than that of the sharp peak and ranged from 0–10 V; its duration was approximately 12 msec. The amplitude of sinusoids from the function generator ranged from 0 – 2 V and frequency was held constant at 500 Hz. The output of the amplifier for sinusoids was 0 – 5.74 V. Single periods of the sinusoid were delivered with intervals in excess of 1 second for single presentation experiments or with intervals corresponding to 10 Hz stimulation. The shape of the stimulus artifact waveform in our patch recordings was qualitatively identical to the first derivative of coil input current waveform, consistent with it resulting from magnetic induction.

D. Animal handling and tissue preparation

Electrophysiological recordings were performed using brain slices prepared from 17–30 days old mice (C57BL/6J; Jackson Laboratory, Bar Harbor, ME). The care and use of animals followed all federal and institutional guidelines, and the Institutional Animal Care and Use Committees of the Boston VA Healthcare System and the Subcommittee of Research Animal Care of the Massachusetts General Hospital. The mice were deeply anesthetized with isoflurane and decapitated. The brains were removed immediately after death and a section of the brain containing the PFC (~1.7 mm anterior to the bregma) and M1 (~0.74 mm anterior to the bregma) was isolated on ice in a 0–5°C oxygenated solution containing (in mM) 1.25 NaH_2PO_4, 2.5 KCl, 25 $NaHCO_3$, 1 $MgCl_2$, 25 glucose, and 225 sucrose, equilibrated with 95% O_2-5% CO_2 (pH 7.4). This cold solution, with a low sodium ion and without calcium ion content, improved tissue viability. In the same medium, 300–400 μm thick coronal slices were prepared using a vibrating blade microtome (Vibratome 3000 Plus, Ted Pella, Inc., Redding, CA) and were incubated at room temperature in an artificial cerebrospinal fluid (aCSF) solution containing (in mM) 125 NaCl, 1.25 NaH_2PO_4, 2.5 KCl, 25 $NaHCO_3$, 1 $MgCl_2$, 2 $CaCl_2$, and 25 glucose, equilibrated with 95% O_2-5% CO_2 (pH 7.4). After a two hour recovery period, slices that contained the PFC and/or M1 were transferred and mounted, caudal side down, to a plastic recording chamber (RC-27L, Warner Instruments, LLC, Hamden, CT) with a plastic slice anchor (SHD-27LP/2, Warner Instruments). The chamber was maintained at 30±2°C, and continuously superfused (3.3 ml/min) with oxygenated aCSF solution.

E. Electrophysiology

PFC or M1 L5 PNs were targeted under visual control. Spiking was recorded with a patch electrode (4–8 MΩ) that was filled with superfusate and positioned onto the surface of a targeted PN (cell-attached mode). Two silver-chloride-coated wires served as the ground and were positioned at opposite edges of the recording chamber, each approximately 15 mm from the targeted cell. The micro-coil assembly was fixed in the micromanipulator such that the central axis of the coil was parallel to the top surface of the brain slice and also perpendicular to the long axis of the targeted PN (c.f. Fig. 2a). The coil assembly was lowered into the bath until the coil was 100 μm above the brain slice surface.

In some experiments, 10 μM 6-cyano-7-nitroquinoxalene -2,3-dione (CNQX) and/or 50 μM D-2-amino-5-phosphonopentanoic acid (D-AP5) were added to the perfusion bath to block AMPA/Kainate and NMDA channels respectively. Both drugs were purchased from Sigma-Aldrich (Sigma-Aldrich Corp., St. Louis, MO). Drugs were prepared daily from concentrated stock solutions; deionized water was added to dilute stock solutions to the appropriate concentration shortly before application.

F. Data Analysis

Raw waveforms were recorded at a sample rate of 100 kHz and processed with custom software written in MATLAB. Many elicited responses contained a series of action potentials (spikes); these were confirmed as spikes by comparing them to those spikes elicited spontaneously. The timing of individual spikes was determined with a ‘matched filter’ - the average spontaneous spike was cross-correlated with the response waveform; peaks in the cross correlation were used to assign timing of individual spikes [13].

In all statistical analyses unpaired t-tests were used to assess whether the difference between the average values for different stimulation conditions was significant. Differences associated with P values <0.1 were regarded as statistically significant. Variances are reported as standard deviation, ±S.D., or standard error, ±S.E.

III. RESULTS

A. Direct measurement of cortical L5 pyramidal neurons to magnetic stimulation

Much previous work with electric stimulation of axons indicates that the effectiveness of a given stimulus is determined by the strength of the gradient of the induced E-field along the length of the axon [21, 22]. Therefore, we built a computational model (Methods) that allowed us to qualitatively visualize how the gradient changed for different orientations of the micro-coil (Fig. 1). Consistent with electromagnetic theory as well as with previous transcranial magnetic stimulation (TMS) studies [23, 24], the strongest gradient arose when the central axis of the coil was held parallel to the surface of the slice and also perpendicular to the long axis of the PN (Figs. 1a and b, top) suggesting that this orientation would be optimal for use in physiological experiments with coronal brain slices in which the apical dendrite and proximal axon were parallel to the slice surface.

We measured responses of L5 PNs from the PFC or M1 to magnetic stimulation from a micro-coil with the orientation of the coil as in the top panel of Figure 1a (Methods); spikes arising from stimulation were recorded using a cell-attached patch clamp electrode positioned on the soma of targeted PNs (Fig. 2a). The results below are derived from recordings in 103 cells (43 different slices). The height of the coil was fixed 100 μm above the surface of the slice for all experiments and the distance from the proximal edge of the coil to the soma of the targeted PN was initially set to 100 μm. As expected, the electrical artifacts arising from both pulsatile and sinusoidal stimulation closely matched the time derivative of the input waveform (Fig. 2b). Despite success with the identical micro-coil in previous studies [12, 13, 25], neither single pulses nor single periods of a 500 Hz sinusoidal waveform were effective for eliciting spiking in L5 PNs (n=15/15, not shown). Because the peak strength of the electric field gradient was not uniform along the length of the coil (Fig. 1b, top) we translated the coil so that its proximal edge was over the soma or as far as 500 μm away but all coil locations were similarly ineffective. Stimuli were delivered at ~40 V, the largest amplitude that could be repeatedly delivered to the coil without overheating [12, 13, 25], resulting in a peak magnetic field strength of 0.3 T, a peak electric field strength of 10.7 V/m and a peak field gradient of 23 kV/m^2. Thus, our results suggest that the threshold for activation of L5 PNs *in vitro* exceeds these levels.

B. Repetitive stimulation is highly effective

In contrast to single pulses or sinusoids, repetitive trains of stimuli were highly effective for eliciting activity. For example, when single periods of a 500 Hz sinusoid were delivered at a rate of 10 Hz for a duration of 4 s (40 total pulses; timing shown at the top of Fig. 2c), robust spiking was elicited soon after the onset of stimulation (Fig. 2c, middle and bottom). Once activated, each stimulus elicited a spike for rates up to 10 Hz; the spike latencies were typically 5 – 10 ms. Spiking persisted throughout the duration of the stimulus in both PFC (n=9/9) and M1 (n=9/9) PNs, even if the duration was extended to 30 s (Figs. 2d) suggesting prolonged stimulation does not desensitize L5 PNs. Increases to the amplitude of stimulation resulted in stronger responses (n=6, Figs. 2e, f) with mean and peak firing rates comparable to the rates of spiking observed during *in vivo* testing [26, 27]. Responses were not significantly altered by the application of either 10 μM 6-cyano-7-nitroquinoxalene-2,3-dione (CNQX), an antagonist of AMPA/Kainate receptors (n=4, not shown) or 50 μM D-2-amino-5-phosphonopentanoic acid (D-AP5), an antagonist of NMDA channels, (n=6, not shown), indicating that spiking responses arising in the proximal axon of the PN were not secondary to the activation of one or more presynaptic neurons.

C. Probing sensitivity along the axon

We explored the effect of translating the coil along the proximal axon and found that thresholds were generally low for coil locations close to the soma and increased as the coil was moved away (Fig. 3a). Interestingly, there was a sudden ‘jump’ in threshold (arrows) that always occurred at the same location for all cells of a given type (PFC: n=6/6; M1: n=6/6), although it occurred at different locations for PFC vs. M1 PNs. It is likely that the different locations arise from differences in the axon trajectories for cells in each of the two cortices. Specifically, the axon emerges from the soma and runs parallel to the top surface of the coronal slice in both types but bends ‘down’ and descends into the slice at a different

location for each. In the PFC, axons bend at a distance of ~150 μm from the soma [28, 29] while in M1 the bend occurs further away, at a distance of ~300 μm [30]. Thus, the persistence of low thresholds for longer distances from the soma in M1 likely reflects the fact that the M1 axon remains in closer proximity to the coil for larger distances from the soma.

Plots of estimated field and field-gradient (Methods) as a function of coil location (Figs. 3b & 3c for PFC and M1 PNs, respectively) reveal that low thresholds arise when the peak of the field-gradient was over the proximal axon (prior to the bend). For example, compare the gradients and thresholds for the PFC PN of Figure 3b at 100 vs. 400 μm or for the M1 PN at 100 vs. 500 μm (Fig. 3c). The jumps in threshold (Fig. 3a, arrows) arise as the peak gradient moves out beyond the bend. Figures 3b & 3c also reveal that thresholds were less well correlated to the strength of the field itself, e.g. in M1, thresholds remained approximately constant for coil locations ranging from 0–300 μm even though the strongest portion of the field moved further and further from the center of the proximal axon (compare field profiles to the left of the dotted vertical line for distances of 0–300 μm).

D. Apical dendrite is also sensitive to magnetic stimulation

Because some previous reports suggest that portions of gray matter may also be sensitive to electrical stimulation [10, 15, 31] we explored whether coil locations over the apical dendrite of L5 PNs might similarly be effective (experimental schematic in Fig. 4a). In our initial testing, neither single stimuli (pulses or sinusoids) nor repetitive trains (durations of 4 or 30 s) were effective (not shown). However, in some of these early experiments, we noticed that the cell began to spike vigorously if several trains of stimulation were delivered in fairly rapid sequence. Therefore, we modified the stimulus protocol to repetitively deliver 30 s periods of stimulation at 10 Hz separated by 20 s intervals so that the effects of prolonged stimulation could be systematically tested. With this paradigm, all PNs became highly responsive (PFC: n=34; M1: n=13). For example, in the PFC PN of Figure 4b (1st row), the onset of spiking occurred midway through the second 30 s period of stimulation, e.g. after ~450 stimuli had been delivered. Similar types of responses can be observed for the other cells in Figure 4b as well (rows 2–4). Brief spiking was sometimes observed during the initial 30-second stimulation interval (Fig. 4b, oblique arrows) but these responses were typically weak and inconsistent and as such were easily distinguished from the onset of continuous spiking that occurred during ensuing stimulation sessions.

The amplitude of the spikes arising from stimulation over the apical dendrite was considerably larger than that arising from stimulation over the proximal axon (compare spike amplitudes in Fig. 4b to those in Fig. 2c). We did not explore the reasons for these differences but parallels to earlier studies [32–35] suggest that the larger spikes may be indicative of a somatic spike while smaller spikes arise from back propagation of an axonal spike to the soma without initiation of a somatic spike. Prolonged stimulation delivered over the proximal axon never initiated similar patterns of delayed-onset, high-amplitude spiking.

Interestingly, two types of responses arose from stimulation over the apical dendrite. Some cells, referred to as Type I, exhibited strong spiking that persisted after the cessation of stimulation (Fig. 4b, 1st and 3rd traces, downward arrows indicate periods of persistent

spiking). In contrast, the response levels in Type II PNs were generally weaker and ended abruptly after termination of the stimulus (Fig. 4b, 2nd and 4th traces). There was little difference in the number of stimulus presentations required to initiate activation between the two types (Fig. 4c, PFC: compare columns 1 and 2, p=0.60; M1: compare columns 3 and 4, p=0.76) although the sensitivity to stimulus amplitude was different for each (Fig. 4d): Type I responses peaked at relatively low stimulation amplitudes (2.86 V) and decreased with further increases in amplitude (n=6), whereas Type II responses increased monotonically (n=5) for the entire range of amplitudes tested here. PNs from the PFC generally required more presentations of the stimulus to initiate spiking than did M1 PNs although the differences were not statistically significant (Fig. 4c, 731.26 +/− 85.14 vs. 479.25 +/− 104.24, p=0.14, unpaired t-test). Although we did not rigorously characterize the morphological properties of the two types of PNs, Type I PNs consistently had large somas (>25 μm) and their apical dendrites appeared thicker and tufted while Type II somas were smaller (<20 μm) and the apical dendrites appeared thinner. This suggests that our Type I PNs correspond to pyramidal tract neurons (PTNs) while Type IIs correspond to intratelencephalic neurons (ITNs) [17, 36]. Consistent with previous findings, type I PNs were considerably more prevalent in PFC cortex but only slightly more prevalent in M1 [37, 38] (Fig. 4e).

E. Does persistent stimulation over the apical dendrite induce a change in state?

The sudden onset and prolonged continuation of vigorous spiking in L5 PNs suggests a change in the underlying state of the PN. Consistent with this notion, once a PN began to spike in response to stimulation over the apical dendrite, its sensitivity to further stimulation was significantly increased. We measured the number of stimuli needed to re-initiate spiking in an ‘activated’ PN and found a dramatic reduction when compared to a ‘naïve’ PN (one that had not yet been stimulated). Whereas, naïve PNs typically required > 400 stimuli to induce robust spiking (Fig. 4c, columns 1–4), activated PNs required only ~15 (Fig. 4c, column 5). Once activated, all L5 PNs tested remained in a state of enhanced sensitivity for the duration of the experiment (range: 30 – 96 min) (n=10). The change in state was observed in both types of PNs and from both cortices suggesting such an effect may be an intrinsic feature of all L5 PNs. Trains with shorter durations (4 s), i.e. the intermittent pattern used in Figure 2c, also brought PNs to the activated state but required a higher number of presentations to initiate onset (1375 +/− 190; Fig. 4c, 6th column).

Responses to stimulation over the apical dendrite were not sensitive to 10 μM CNQX and the number of stimuli required to induce the change in state was also not affected (Fig. 4f, p=0.29 for type I; p=0.36 for type II, two-tailed t-test). Responses were completely eliminated however when 50 μM D-AP5 was included with the CNQX (n=6, not shown). Thus, the response to stimulation over the apical dendrite arises secondary to activation of one or more local excitatory neurons and further, is mediated via the delivery of glutamate through NMDA receptors. Spiking responses were restored when the CNQX/AP5 cocktail was washed out.

F. Position-dependent sensitivity of the apical dendrite

Similar to the maps for the proximal axon, we measured the threshold required to induce a state change as the coil was stepped along the apical dendrite; the proximal edge to soma distance ranged from 0 (adjacent to soma) to 500 μm (corresponding to the superficial border of layer 1). We found that coil locations closer to the soma had higher sensitivity than more distal locations (Fig. 4g, compare dashed and solid lines) although there was not a sharp transition in threshold as was observed for stimulation over the proximal axon. The consistent increase in threshold with increasing distance from the soma suggests that the presynaptic neurons activated by stimulation are situated closer to the proximal portion of the apical dendrite. In Type I PNs (circular symbols), stimulation with the proximal edge of the coil over the soma and even 100 μm over the proximal axon did not induce spiking during the stimulus but instead generated a robust response at stimulus offset; these 'OFF responses' were not included in the threshold map of Figure 4g. Thresholds maps along the apical dendrite were also re-measured for PNs that had previously been activated and revealed the lowest thresholds of this study (Fig. 4g, triangle). For example, threshold reductions at a location of 100 μm were 77 % and 47 % of those in non-activated cells for Type I and II PNs respectively. For comparison, the horizontal dashed line indicates the minimum thresholds arising from the axonal stimulation experiments of Figure 3a.

G. Coil alignment influences responsiveness

Responses in L5 PNs were highly sensitive to the alignment between the induced electric field and the orientation of the PN. For example, when the coil was rotated so that its central axis was brought parallel to the long axis of the PN while still remaining parallel to the surface of the slice (alignment shown in Fig. 1a, middle panel), there was a complete loss of responsiveness (n=18; Fig. 5a, bottom) - even a 5–10x increased in the number of presentations was not effective (range: 6,000–12,000). While this is consistent with the weaker fields and gradients associated with direct activation for this orientation of the cell (Fig. 1), it was somewhat surprising that prolonged stimulation of horizontally oriented processes (or axons) was also not effective. Interestingly, oblique orientations of the coil (Fig. 5a, middle) led to an 'OFF' type of response, e.g. no spikes generated during the stimulus but strong spiking arose after its termination (n=12). Further, delivery of obliquely-oriented stimuli to PNs that had previously been activated resulted in a more substantial 'OFF' response than that which occurred in naïve PNs (Fig. 5b, left panels). Adjusting the coil to the standard perpendicular orientation (Fig. 5b, right, top) converted the OFF response back to ON (Fig. 5b, right panels). Even though oblique coil orientations did not initiate spiking per se, they were still effective for bringing naïve PNs into the activated state and required a similar number of presentations to that from the perpendicular orientation (Fig. 5c, 2nd and 4th column).

H. Control experiments

To determine whether the neural responses and the state changes observed in this study were indeed elicited by magnetic stimulation, we performed a series of control experiments that were similar to those done in earlier studies [12, 13].

First, to minimize the possibility of capacitive currents as a source of activation the 'return' electrode in these experiments was not situated in a way that forced the capacitive current through the targeted tissue as it was in a previous study that demonstrated capacitive activation of retinal neurons [39]. As such, any capacitive effects would be limited to only the immediate vicinity of the coil. Further, the distance in the previous study between the retina and the capacitive supply was 0.03 μm, much closer than the 100 μm separation used here.

To further ensure that capacitive current was not contributing to activation, we applied strong current transiently to 'burn out' a small portion of the coil. Effective burning caused an increase in impedance across the two leads of the coil from about 8 Ω to over 200 MΩ without simultaneously burning through the insulation. In this manner, subsequent delivery of a voltage potential across the coil leads produced a capacitive current across the burnt portion of the coil without providing a path for the flow of electrical current directly into the bath. Use of the 'burnt' coil was never effective for eliciting neural activity, strongly suggesting that capacitive current could be ruled out as a potential source of activation.

We were also concerned that the heating of the coils might lead to thermal activation. However, direct measurement of bath temperature in response to stimulation revealed changes of less than 1°C in response to the stimuli used in our experiments. Briefly, a 30V 100 μs pulse at 1~10Hz for a duration of 30 sec led to a temperature increase of +0.12~0.55°C. 4.3V 2 ms sine waveform at 1~10Hz for a 30 sec duration led to a temperature increase of +0.28~0.96°C. Temperature was measured at a distance of 50 μm from the coil surface while the bath temperature was maintained at 30°C so as to closely match physiological testing conditions. Because the resulting temperature increases were always less than 1°C, it is unlikely that nearby cortical neurons were activated by temperature, e.g., recent wireless magneto-thermal stimulation studies show that mouse cortical neurons were not activated even by a temperature increase of 10 °C [40].

Furthermore, if heat were the underlying mechanism of activation, we would expect coil orientations for which the coil was most closely aligned to the cell to be most effective, e.g. the alignment shown in Figure 1a (middle, left) should be more effective than the other coil orientations (top or bottom panels). However, the opposite was true. The complete inability to induce spiking with the orientation of the middle panel but the consistent activation with the orientation shown in the top panel strongly suggests that the induced response is not mediated by thermal transfer from the coil to the cell.

The state changes observed here could persist for periods up to 30 minutes after onset and once initiated could persist without additional stimulation. Because the high rate of perfusion helped to ensure any increases in temperature would be highly transient, a sustained change in state could not be mediated by any transient increases in temperature. Further, as described above in the control experiments certain orientations of the coil did not induce state changes even though a larger portion of the coil mass was in closer proximity to the cell; this lends further support that temperature was not the underlying cause of the state change.

IV. DISCUSSION

While much previous work has shown that the axon and especially the AIS have high sensitivity to electric stimulation [10, 14, 21, 22, 41], here we found that portions of the apical dendrite of L5 PNs may have even higher sensitivity, especially under conditions of repetitive stimulation. Prolonged stimulation led to a change in the state of the neuron with a corresponding increase in sensitivity. In the activated state, thresholds for activation of the apical dendrite were ~ 35 % lower than the lowest thresholds found for stimulation over the proximal axon. As part of this work, we found that PNs can be activated by relatively weak electric fields, at least during repetitive stimulation. The peak field strength arising during the repetitive stimulation protocol used here was estimated to be ~0.05 V/m (explicit conversion factor for 500 Hz sine waveform: ~0.0125 V/m per 1V amplitude) – much lower than many previous estimates of threshold [23, 24, 42]. Both the current and voltage levels used here are higher than those used in previous studies with electric stimulation and thus it will be important to consider this requirement during further evaluation of coils.

We also found that coil orientation plays a critical role in the activation of cortical pyramidal neurons and that slight shifts in orientation can convert elicited spiking into an ‘OFF’ response, i.e. dormant during stimulation but robust after termination of the stimulus. Thus, carefully oriented arrays of coils may enable the creation of very precise patterns of neural activity, e.g. ones in which different types of cortical neurons can be individually activated or suppressed, and therefore may facilitate closer matches to key elements of physiological signaling patterns. Finally, although it is well established that activation of either horizontal processes or horizontal axons can induce a response in pyramidal neurons [9, 10]; here we found that a given stimulus, capable of robustly activating the PN when oriented along the axonal axis, was ineffective when oriented horizontally, even when many thousands of repetitions were delivered. This provides additional support that certain coil orientations may be effective for confining stimulation to a focal region around the coil.

Our results also provide new insights into findings from previous *in vivo* cortical stimulation studies. For example, our sensitivity measurements along the proximal axon and apical dendrite may provide an alternative explanation for the discrepancy between the earlier studies of DeYoe et al [15] and Tehovnik et al [14, 43]. Both groups measured thresholds as a function of the depth of penetration of a stimulating electrode inserted into V1 in awake, behaving non-human primates (NHPs) but the depths at which thresholds were lowest were different for the two groups. Tehovnik and colleagues found the lowest thresholds when the tip of the stimulating electrode was close to L6 while the DeYoe study found thresholds were lowest at more superficial locations (L2/3). L5 PNs in V1 provide a strong projection to the superior colliculus [17, 44] and are known to mediate saccades (the detection criteria used in the Tehovnik study); thus, the low thresholds we observed here for coil locations over the proximal axon, corresponding approximately to L6, support the findings of the Tehovnik group. However, our finding of low thresholds for coil locations over the apical dendrite (L2/3–L4), especially after prolonged stimulation, are also consistent with the low threshold regions observed by DeYoe. Interestingly, the duration of the stimulus trains used by DeYoe were much longer than those used by the Tehovnik group and might therefore have facilitated a change in state similar to the one observed here. Further, the

psychophysical detection criteria used by DeYoe may have involved higher regions of visual cortex; if so, activation of L2/3 pyramidal neurons would have been required since their axons form the principal projection to secondary visual cortex (V2) [45]. Taken together, these results raise the possibility that different parameters of stimulation may be optimal for each depth of penetration and further, stimulation parameters and depth can combine to significantly alter the elicited patterns of neural activation. Improved understanding of these relationships will be especially important for applications where the creation of more precise patterns of neural activity may be necessary, e.g. devices that target sensory cortices [3]. Note that our results do not preclude the possibility that a breakdown in electrode efficacy in the DeYoe study contributed to the different results described above.

It is important to point out however that many synaptic connections to the pyramidal neurons studied here were necessarily lost during preparation of the brain slice and therefore the relative sensitivity along pyramidal neurons in the intact brain may be different than what was found here. Also, myelin formation is still under development in the 17–30 day old mice used in this study and thus the sensitivity profile in adult animals may have further differences.

The change in state measured here at the single cell level *in vitro* has some strong similarities to the state changes described in previous psychophysical and electrophysiological studies *in vivo* [10, 18, 19]. For example, both require an extended period of stimulation, both are associated with a significant reduction in threshold and both exhibit responses that persist beyond the duration of the stimulus [10, 18, 19]. These similarities raise the possibility that the state change in L5 PNs observed here may be the neuronal correlate of many of the *in vivo* state changes reported previously. The state changes found here *in vitro* were observed in all cortical regions tested including PFC and M1 as well as a few additional L5 PNs from somatosensory cortex (not shown) and therefore, suggest that the ability to change state may be a general property of all cortical pyramidal neurons – or at least those of Layer 5. Because the brain slice preparation used here severs most long-distance synaptic connections, our results further suggest that computation of state occurs within a local region of cortex and thus imply that state changes can occur without contributions from subcortical brain regions as have been suggested previously [10, 19]. Nevertheless, our experiments do not rule out the possibility that additional brain circuits may contribute *in vivo*.

State changes were eliminated in the presence of D-AP5, indicating that synaptic input, mediated through NMDA receptors on the apical dendrite of L5 PNs, is required. Our results do not reveal the presynaptic neuron activated by stimulation but the PNs of layer 2/3 and simple cells (i.e. excitatory stellate cells) of layer 4 are the most likely candidates. Both are situated upstream of the L5 PN [46], both are glutamatergic and both are oriented perpendicularly to the cortical surface and therefore, their expected sensitivity to coil orientation matches the results found here. Final support for these two candidates comes from our finding of peak sensitivity at L4, i.e. the highest sensitivity occurred when the peak of the field-gradient was situated over the highly-sensitive axon initial segment (AIS) of both neurons. It will be interesting in future studies to ascertain whether the state changes observed here are correlated to specific markers of synaptic plasticity.

In addition to its potential as a neural prosthetic, our results raise the possibility that implanted micro-coils may also be useful for studying the neural mechanisms underlying rTMS. The small fields from micro-coils confine activation to a focal portion of the animal brain (analogous to the situation during human rTMS) and also may preclude the need for anesthesia, thereby avoiding the block of NMDA channels associated with some anesthetics and the corresponding inability to induce state changes [47]. Implanted micro-coils would be conducive to systematic testing of different rTMS paradigms and might therefore help to identify factors that contribute to the high levels of variability observed across rTMS studies [48, 49]. For example, different depths of implantation might allow different pyramidal neurons to be separately targeted thereby allowing the contribution of each to the rTMS response to be dissected. It is interesting to note that the number of stimuli delivered in many common rTMS protocols [48, 49] is comparable to the number of stimuli needed here to induce the change in state as this raises the possibility that a change in state of L5 PNs may underlie the effectiveness of some rTMS protocols. Further, the fact that very weak electric fields can induce activity has considerable implications for understanding the mechanisms of repetitive TMS (rTMS) [48] as they raise the possibility that activation from a given stimulus may occur over a much wider region than previously thought. Small coils would be less suitable for unraveling the mechanisms of single pulse TMS and other types of questions where the spatial properties of the induced waveform play a more critical role.

Several significant obstacles will need to be overcome before clinical implementation of micro-coils can be considered viable. For example, although a direct spike could be elicited for each stimulus the maximum stimulus rate that could be delivered with this coil was limited to 10 Hz. While this may be sufficient to reproduce some elements of physiological signaling [26, 27], the rates used previously to induce phosphenes and/or saccades during electric stimulation were considerably higher [14, 15]. A second important limitation is that high levels of current (> 178 mA) were necessary to induce the fields required for activation and thus the power levels associated with magnetic stimulation from micro-coils are greater than those associated with electric stimulation [13]. Lower levels of current will also be necessary to enable faster rates of stimulation to be delivered without burning the micro-wires that comprise the coil. Innovative coil winding schemes may help to enhance the strength of the induced fields and should lead to a corresponding reduction in power levels as well but it is not clear just how much reduction can be obtained. The use of ferrite or other field-enhancing cores should dramatically increase field strength and reduce power levels. Such cores may also help to significantly reduce coil sizes to a level that minimizes the damage to cortex resulting from implantation. Chronic implantation studies will also be needed to ensure that magnetic stimulation has no untoward effect on the surrounding tissue although this does not seem likely given the much stronger fields delivered from TMS. Finally, although the state change resulting from prolonged stimulation may be useful for increasing the overall sensitivity of cortical neurons to future stimulation, the relatively large latencies associated with spiking onset, even in activated neurons raises questions about whether stimulation of the apical dendrite will be useful for replicating the temporal components of neural signals. It will nevertheless be interesting in future studies to explore whether the change in state can be harnessed to increase the overall efficacy of stimulation.

References

1. Schmidt EM, Bak MJ, Hambrecht FT, Kufta CV, O'Rourke DK, Vallabhanath P. Feasibility of a visual prosthesis for the blind based on intracortical microstimulation of the visual cortex. Brain. Apr; 1996 119(Pt 2):507–22. [PubMed: 8800945]
2. Tehovnik EJ, Slocum WM. Electrical induction of vision. Neurosci Biobehav Rev. Jun.2013 37:803–18. [PubMed: 23535445]
3. Bensmaia SJ, Miller LE. Restoring sensorimotor function through intracortical interfaces: progress and looming challenges. Nat Rev Neurosci. May.2014 15:313–25. [PubMed: 24739786]
4. Polikov VS, Tresco PA, Reichert WM. Response of brain tissue to chronically implanted neural electrodes. J Neurosci Methods. 2005; 148:1–18. [PubMed: 16198003]
5. Koivuniemi A, Wilks SJ, Woolley AJ, Otto KJ. Multimodal, longitudinal assessment of intracortical microstimulation. Prog Brain Res. 2011; 194:131–44. [PubMed: 21867800]
6. Davis TS, Parker RA, House PA, Bagley E, Wendelken S, Normann RA, Greger B. Spatial and temporal characteristics of V1 microstimulation during chronic implantation of a microelectrode array in a behaving macaque. J Neural Eng. Dec.2012 9:065003. [PubMed: 23186948]
7. Bradley DC, Troyk PR, Berg JA, Bak M, Cogan S, Erickson R, Kufta C, Mascaro M, McCreery D, Schmidt EM, Towle VL, Xu H. Visuotopic mapping through a multichannel stimulating implant in primate V1. J Neurophysiol. Mar.2005 93:1659–70. [PubMed: 15342724]
8. Grill WM, Norman SE, Bellamkonda RV. Implanted neural interfaces: biochallenges and engineered solutions. Annu Rev Biomed Eng. 2009; 11:1–24. [PubMed: 19400710]
9. Histed MH, Bonin V, Reid RC. Direct activation of sparse, distributed populations of cortical neurons by electrical microstimulation. Neuron. Aug 27.2009 63:508–22. [PubMed: 19709632]
10. Histed MH, Ni AM, Maunsell JH. Insights into cortical mechanisms of behavior from microstimulation experiments. Prog Neurobiol. Apr.2013 103:115–30. [PubMed: 22307059]
11. McCreery D, Pikov V, Troyk PR. Neuronal loss due to prolonged controlled-current stimulation with chronically implanted microelectrodes in the cat cerebral cortex. J Neural Eng. Jun.2010 7:036005. [PubMed: 20460692]
12. Bonmassar G, Lee SW, Freeman DK, Polasek M, Fried SI, Gale JT. Microscopic magnetic stimulation of neural tissue. Nat Commun. 2012; 3:921. [PubMed: 22735449]
13. Lee SW, Fried SI. Suppression of subthalamic nucleus activity by micromagnetic stimulation. IEEE Trans Neural Syst Rehabil Eng. Jan.2015 23:116–27. [PubMed: 25163063]
14. Tehovnik EJ, Slocum WM. Depth-dependent detection of microampere currents delivered to monkey V1. European Journal of Neuroscience. Apr.2009 29:1477–89. [PubMed: 19519630]
15. DeYoe EA, Lewine JD, Doty RW. Laminar variation in threshold for detection of electrical excitation of striate cortex by macaques. J Neurophysiol. Nov.2005 94:3443–50. [PubMed: 16079194]
16. Im M, Fried SI. Indirect activation elicits strong correlations between light and electrical responses in ON but not OFF retinal ganglion cells. J Physiol. Aug 15.2015 593:3577–96. [PubMed: 26033477]
17. Molnar Z, Cheung AF. Towards the classification of subpopulations of layer V pyramidal projection neurons. Neurosci Res. Jun.2006 55:105–15. [PubMed: 16542744]
18. Pasley BN, Allen EA, Freeman RD. State-dependent variability of neuronal responses to transcranial magnetic stimulation of the visual cortex. Neuron. Apr 30.2009 62:291–303. [PubMed: 19409273]
19. Silvanto J, Pascual-Leone A. State-dependency of transcranial magnetic stimulation. Brain Topogr. Sep.2008 21:1–10. [PubMed: 18791818]
20. Miranda PC, Hallett M, Basser PJ. The electric field induced in the brain by magnetic stimulation: a 3-D finite-element analysis of the effect of tissue heterogeneity and anisotropy. IEEE Trans Biomed Eng. Sep.2003 50:1074–85. [PubMed: 12943275]
21. Ranck JB Jr. Which elements are excited in electrical stimulation of mammalian central nervous system: a review. Brain Res. Nov 21.1975 98:417–40. [PubMed: 1102064]

22. Rattay F. The basic mechanism for the electrical stimulation of the nervous system. Neuroscience. Mar.1999 89:335–46. [PubMed: 10077317]
23. Maccabee PJ, Amassian VE, Eberle LP, Cracco RQ. Magnetic coil stimulation of straight and bent amphibian and mammalian peripheral nerve in vitro: locus of excitation. J Physiol. Jan.1993 460:201–19. [PubMed: 8487192]
24. Salvador R, Silva S, Basser PJ, Miranda PC. Determining which mechanisms lead to activation in the motor cortex: a modeling study of transcranial magnetic stimulation using realistic stimulus waveforms and sulcal geometry. Clin Neurophysiol. Apr.2011 122:748–58. [PubMed: 21035390]
25. Park HJ, Bonmassar G, Kaltenbach JA, Machado AG, Manzoor NF, Gale JT. Activation of the central nervous system induced by micro-magnetic stimulation. Nat Commun. 2013; 4:2463. [PubMed: 24030203]
26. Lee SH, Kwan AC, Zhang S, Phoumthipphavong V, Flannery JG, Masmanidis SC, Taniguchi H, Huang ZJ, Zhang F, Boyden ES, Deisseroth K, Dan Y. Activation of specific interneurons improves V1 feature selectivity and visual perception. Nature. Aug 16.2012 488:379–83. [PubMed: 22878719]
27. Otani S. Prefrontal cortex function, quasi-physiological stimuli, and synaptic plasticity. J Physiol Paris. Jul-Nov;2003 97:423–30. [PubMed: 15242654]
28. Vertes RP. Interactions among the medial prefrontal cortex, hippocampus and midline thalamus in emotional and cognitive processing in the rat. Neuroscience. Sep 29.2006 142:1–20. [PubMed: 16887277]
29. Gorelova N, Yang CR. The course of neural projection from the prefrontal cortex to the nucleus accumbens in the rat. Neuroscience. Feb.1997 76:689–706. [PubMed: 9135043]
30. Yamawaki N, Shepherd GM. Synaptic circuit organization of motor corticothalamic neurons. Journal of Neuroscience. Feb 4.2015 35:2293–307. [PubMed: 25653383]
31. Nowak LG, Bullier J. Axons, but not cell bodies, are activated by electrical stimulation in cortical gray matter. II. Evidence from selective inactivation of cell bodies and axon initial segments. Exp Brain Res. Feb.1998 118:489–500. [PubMed: 9504844]
32. Hu W, Tian C, Li T, Yang M, Hou H, Shu Y. Distinct contributions of Na(v)1.6 and Na(v)1.2 in action potential initiation and backpropagation. Nature Neuroscience. Aug.2009 12:996–1002. [PubMed: 19633666]
33. Stuart G, Spruston N, Sakmann B, Hausser M. Action potential initiation and backpropagation in neurons of the mammalian CNS. Trends Neurosci. Mar.1997 20:125–31. [PubMed: 9061867]
34. Cai C, Twyford P, Fried S. The response of retinal neurons to high-frequency stimulation. J Neural Eng. Jun.2013 10:036009. [PubMed: 23594620]
35. Mainen ZF, Joerges J, Huguenard JR, Sejnowski TJ. A model of spike initiation in neocortical pyramidal neurons. Neuron. Dec.1995 15:1427–39. [PubMed: 8845165]
36. Lee AT, Gee SM, Vogt D, Patel T, Rubenstein JL, Sohal VS. Pyramidal neurons in prefrontal cortex receive subtype-specific forms of excitation and inhibition. Neuron. Jan 8.2014 81:61–8. [PubMed: 24361076]
37. Kawaguchi Y. Groupings of nonpyramidal and pyramidal cells with specific physiological and morphological characteristics in rat frontal cortex. J Neurophysiol. Feb.1993 69:416–31. [PubMed: 8459275]
38. Gao WJ, Zheng ZH. Target-specific differences in somatodendritic morphology of layer V pyramidal neurons in rat motor cortex. J Comp Neurol. Aug 16.2004 476:174–85. [PubMed: 15248197]
39. Eickenscheidt M, Jenkner M, Thewes R, Fromherz P, Zeck G. Electrical stimulation of retinal neurons in epiretinal and subretinal configuration using a multicapacitor array. J Neurophysiol. May.2012 107:2742–55. [PubMed: 22357789]
40. Chen R, Romero G, Christiansen MG, Mohr A, Anikeeva P. Wireless magnetothermal deep brain stimulation. Science. Mar 27.2015 347:1477–80. [PubMed: 25765068]
41. Fried SI, Lasker AC, Desai NJ, Eddington DK, Rizzo JF. Axonal sodium-channel bands shape the response to electric stimulation in retinal ganglion cells. Journal of Neurophysiology. 2009; 101:1972–1987. [PubMed: 19193771]

42. Parthoens J, Verhaeghe J, Wyckhuys T, Stroobants S, Staelens S. Small-animal repetitive transcranial magnetic stimulation combined with [(1)(8)F]-FDG microPET to quantify the neuromodulation effect in the rat brain. Neuroscience. Sep 5.2014 275:436–43. [PubMed: 24979056]
43. Tehovnik EJ, Slocum WM, Schiller PH. Saccadic eye movements evoked by microstimulation of striate cortex. Eur J Neurosci. Feb.2003 17:870–8. [PubMed: 12603277]
44. Martin KA, Whitteridge D. Form, function and intracortical projections of spiny neurones in the striate visual cortex of the cat. J Physiol. Aug.1984 353:463–504. [PubMed: 6481629]
45. Sincich LC, Horton JC. The circuitry of V1 and V2: integration of color, form, and motion. Annu Rev Neurosci. 2005; 28:303–26. [PubMed: 16022598]
46. Martinez LM, Alonso JM, Reid RC, Hirsch JA. Laminar processing of stimulus orientation in cat visual cortex. J Physiol. Apr 1.2002 540:321–33. [PubMed: 11927690]
47. Ebert B, Mikkelsen S, Thorkildsen C, Borgbjerg FM. Norketamine, the main metabolite of ketamine, is a non-competitive NMDA receptor antagonist in the rat cortex and spinal cord. Eur J Pharmacol. Aug 20.1997 333:99–104. [PubMed: 9311667]
48. Hoogendam JM, Ramakers GM, Di Lazzaro V. Physiology of repetitive transcranial magnetic stimulation of the human brain. Brain Stimul. Apr.2010 3:95–118. [PubMed: 20633438]
49. Pell GS, Roth Y, Zangen A. Modulation of cortical excitability induced by repetitive transcranial magnetic stimulation: influence of timing and geometrical parameters and underlying mechanisms. Prog Neurobiol. Jan.2011 93:59–98. [PubMed: 21056619]

Biographies

Seung Woo Lee was born in Seoul, Korea, in 1979. He received the B.S. degree in school of electrical engineering and computer science from Seoul National University (SNU), Seoul, Korea, in 2003. He received the Ph.D. degree in the school of electrical engineering and computer science from the Seoul National University, in 2010. His Ph.D. degree thesis was on the development of long-term implantable neuroprosthetic devices using Liquid Crystal Polymers.

He was a Research Fellow in the Inter-university Semiconductor Research Center (ISRC) at the Seoul National University until December, 2010. From 2011 to 2015, he was a Research Fellow in the Department of Neurosurgery at Massachusetts General Hospital and Harvard Medical School, Boston, MA, USA. Since November 2015, he has been working as an Instructor in the Department of Neurosurgery at the Harvard Medical School. He is also an Assistant in the Department of Neurosurgery at the Massachusetts General Hospital (MGH). His research interests include development of chronic implantable electronic system (BioMEMs and Bioelectronics) as well as effective electric/magnetic neural stimulation technology (Neurophysiology) for neuroscience research and neural prosthesis.

Shelley I. Fried was born in Brooklyn, New York City, in 1961. He received a B.E degree in Mechanical Engineering from Cooper Union in 1982, an M.S. degree in biomedical engineering from the Pennsylvania State University in 1986 and the Ph.D. degree in vision science from the University of California, Berkeley, in 2004.

From 2004 to 2006, he was a Postdoctoral Fellow in the Molecular and Cell Biology at Berkley and from 2006–2007 he was a Research Fellow at the Massachusetts General Hospital, Department of Neurosurgery. Since 2008, he has been a Research Scientist at the Boston VA Healthcare System and an Associate in Neuroscience at the Massachusetts General Hospital. He is also an Associate Professor in the Department of Neurosurgery at Harvard Medical School. His research interests lie within the field of neural prosthetics with a focus towards understanding the fundamental mechanisms by which neurons respond to artificial stimulation.

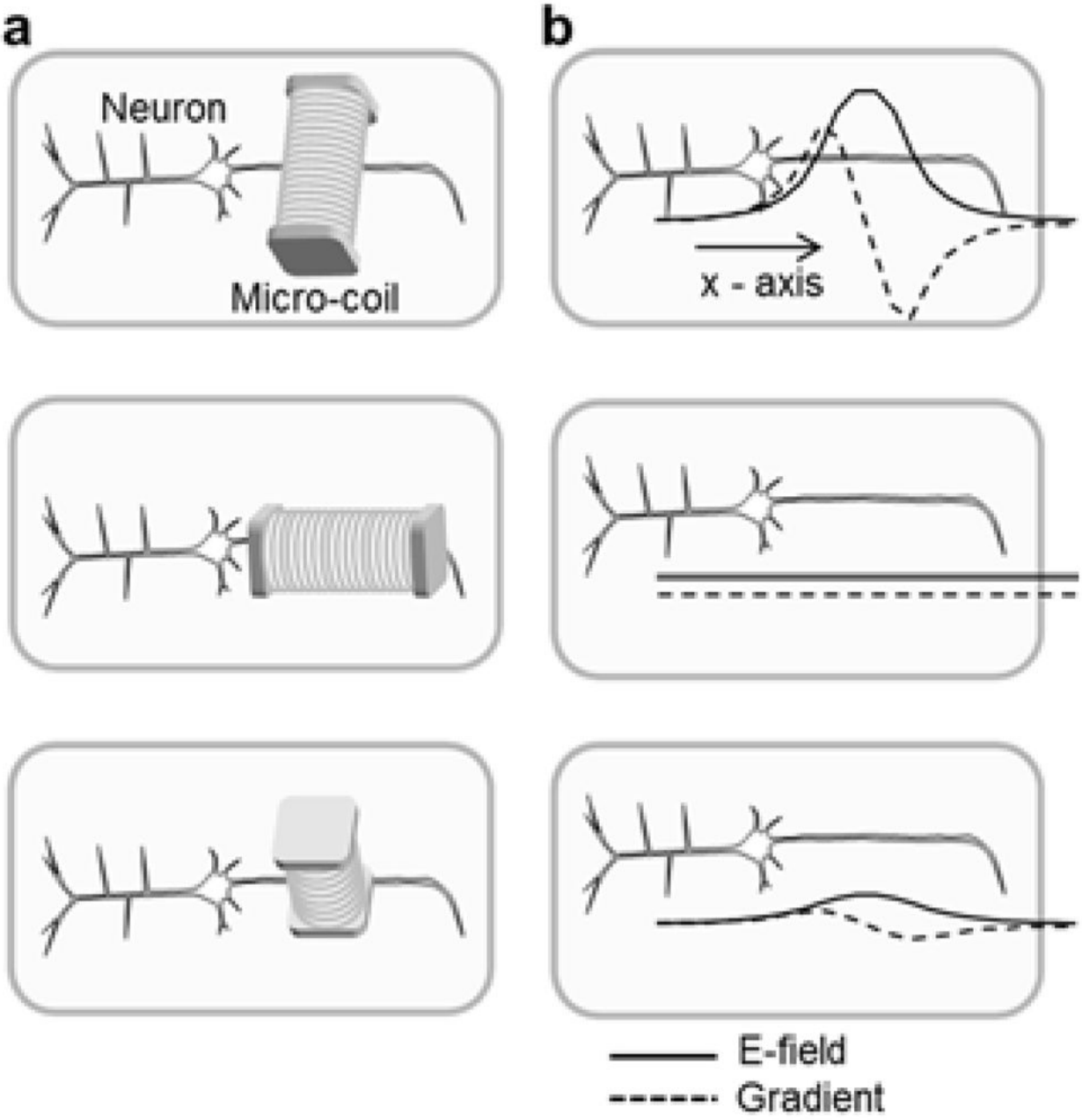

Fig. 1.

Orientation of micro-coils shapes the induced electric field. (a) Schematic diagram of three orthogonal orientations of the micro-coil relative to a targeted cortical pyramidal neuron (PN) within a coronal brain slice. (top) The central axis of the coil is parallel to the surface of brain slice and perpendicular to the axonal axis of the PN. (middle) The central axis of the coil is now parallel to both the brain slice surface and the axonal axis. (bottom) The coil axis is perpendicular to both the brain slice surface and the axonal axis. (b) The magnitude of the induced electric (E) field along the long axis of the PN (solid line) as well as its spatial gradient (dashed line) for each orientation of the coil.

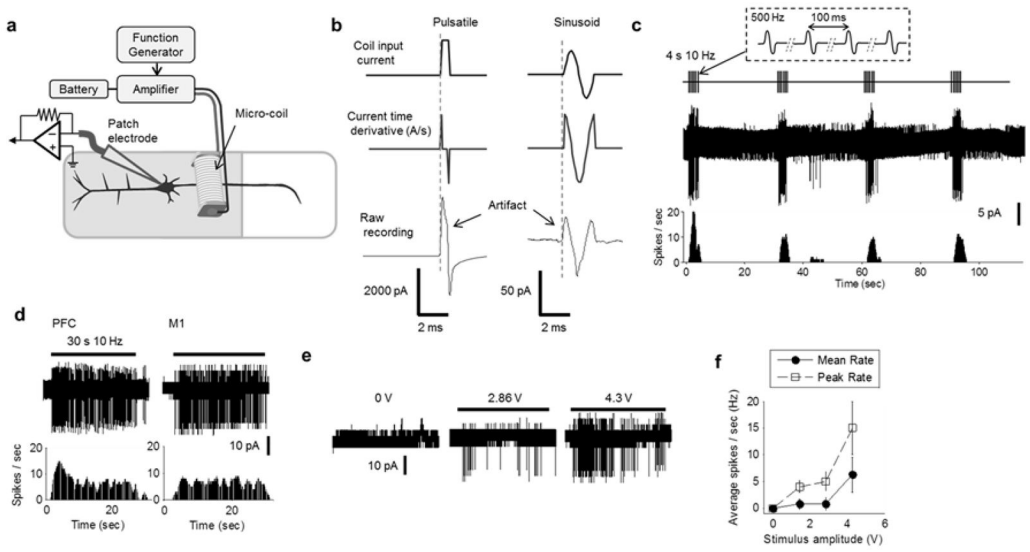

Fig. 2.

The proximal axon is sensitive to magnetic stimulation from a micro-coil. (a) Schematic of the experimental set-up: a patch electrode was used to record spiking from the soma of an L5 PN in response to stimulation from the micro-coil. The bottom edge of the coil was fixed 100 μm above the surface of the slice and the proximal edge (of the coil) was 100 μm from the soma. (b) Stimulation waveforms from pulsatile and sinusoid stimulation. Stimulus artifacts closely matched the time derivative of the coil input waveforms. (c) Responses to repetitive magnetic stimulation. (top) Stimuli consisted of single periods of a 500 Hz sinusoid (inset) delivered at a rate of 10 Hz for 4 s (40 total stimuli). This pattern was repeated every 30 s. (middle) Raw response from a typical L5 PN. (bottom) Corresponding PSTH (binsize = 0.1 s). (d) Responses to 10 Hz stimulation delivered for 30 s (300 total stimuli) from typical PFC and M1 PNs (left and right, respectively); horizontal bars at top indicate the timing of the stimulus. The corresponding PSTH is shown below each trace (binsize = 0.1 s). (e) Responses to different amplitudes of stimulation. Horizontal bars at top represent 10 Hz stimulation for 30 s; the amplitude of the stimulus (in Volts) is indicated above each bar. (f) Average spike rate of L5 PNs (PFC) as a function of stimulus amplitude. Error bars represent standard errors (S.E.; n=6).

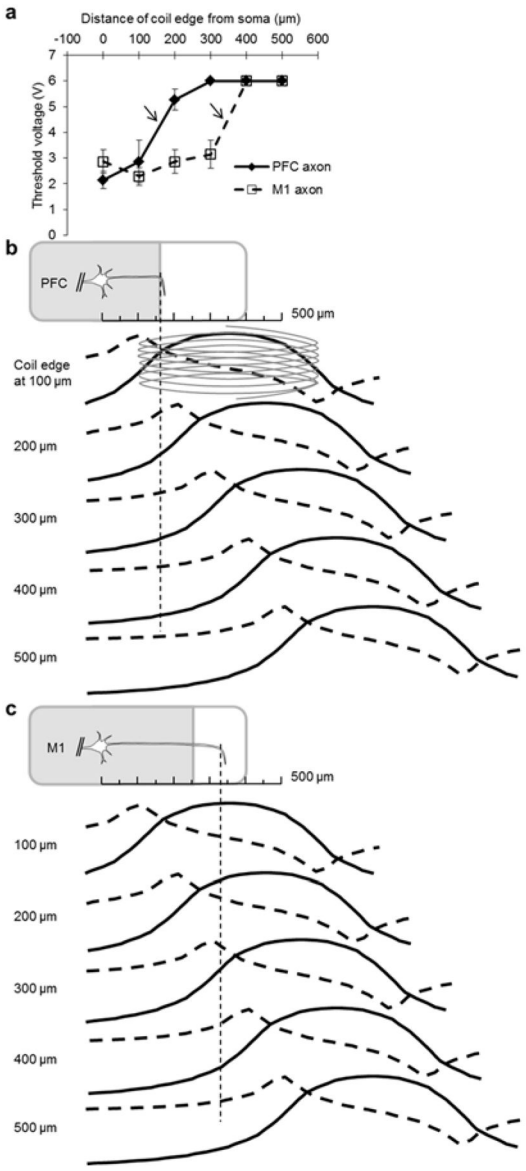

Fig. 3.

Cell type-dependent sensitivity of L5 PNs to stimulation along the axon. (a) Mean threshold of the coil-input voltage needed to elicit spiking in L5 PNs as a function of the distance between the coil edge and the soma (PFC: filled diamond points and solid line (n=9); M1: open square points and dashed line (n=5)). Bars represent S.E. The maximum input voltage to the coil was limited to 6 V so data points at that level underestimate actual thresholds. Arrows indicate a sudden transition in threshold voltage (see text). (b) (top) Schematic illustration of a PFC PN. The axon extends along the plane of the coronal slice but bends into the slice at a distance of ~150 μm from the soma; the thin dashed line indicates the bend location. (lower traces) Each row represents the induced E-field (solid trace) and its spatial gradient (dashed trace) arising from a coil positioned at a different location along the proximal axon (distances are given at left). (c) Analogous to (b) but for M1 PNs. Note the axon bend in M1 PNs occurs further from the soma.

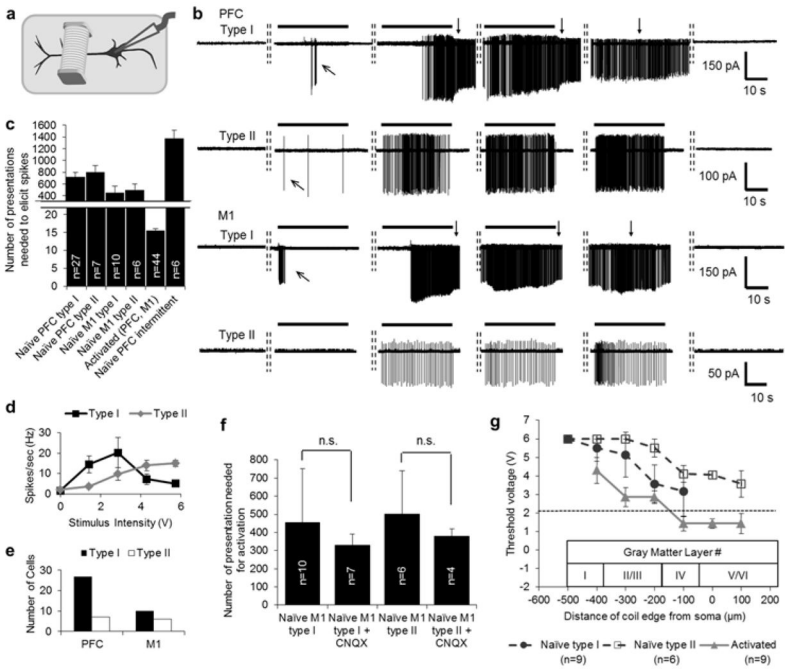

Fig. 4.

Stimulation of the apical dendrite activates L5 PNs. (a) Schematic indicating the coil positioned over the apical dendrite. (b) Responses to 10 Hz stimulation from a coil that was 100 μm from the soma; horizontal bars above each response represent a 30 s period during which stimulation was applied (300 total stimuli). Rows 1–2 are from PFC PNs and rows 3–4 from M1 PNs. Rows 1 & 3 are Type I PNs and rows 2 & 4 are Type II (see text). The dashed vertical lines between traces indicate 20 s intervals between consecutive periods of stimulation. Downward pointing arrows in rows 1 & 3 indicate periods of burst firing that persisted after the end of a stimulus train. Oblique arrows indicate transient spiking that sometimes occurred prior to the onset of continuous spiking. (c) Average number of presentations required to elicit spiking onset in different types of PNs; stimulus is repetitive 10 Hz, 30 s duration, 20 s interval for five left-most bars and 10 Hz, 4s duration, 26 s interval for right-most bar. Error bars represent S.E. (d) Average spike rate of the two types of PNs as a function of stimulus amplitude (type I, n=6; type II, n=5). (e) Distribution of the two types of PNs in PFC and M1 cortices. (f) Average numbers of presentations needed for activation of PNs in control vs. 10 μM CNQX. Unpaired t-test indicates the differences were not statistically significant (Type I: p=0.29; Type II: p=0.36). Error bars indicate standard deviation (±S.D.). (g) Mean thresholds to elicit spikes as a function of the distance between the soma and the closest edge of the coil to the soma (all locations over the apical dendrite). Coil height was fixed at 100 μm above the slice surface. Stimulation was 10 Hz for 30 s. Dark filled circles: naïve type I PNs; open squares: naïve type II; shaded triangles: activated PNs. Bars represent S.E. Data points at 6 V indicate the threshold exceeded the upper limit of the stimulus system. The dashed horizontal line indicates the minimum threshold for stimulation over the axon (cf. Fig. 3a).

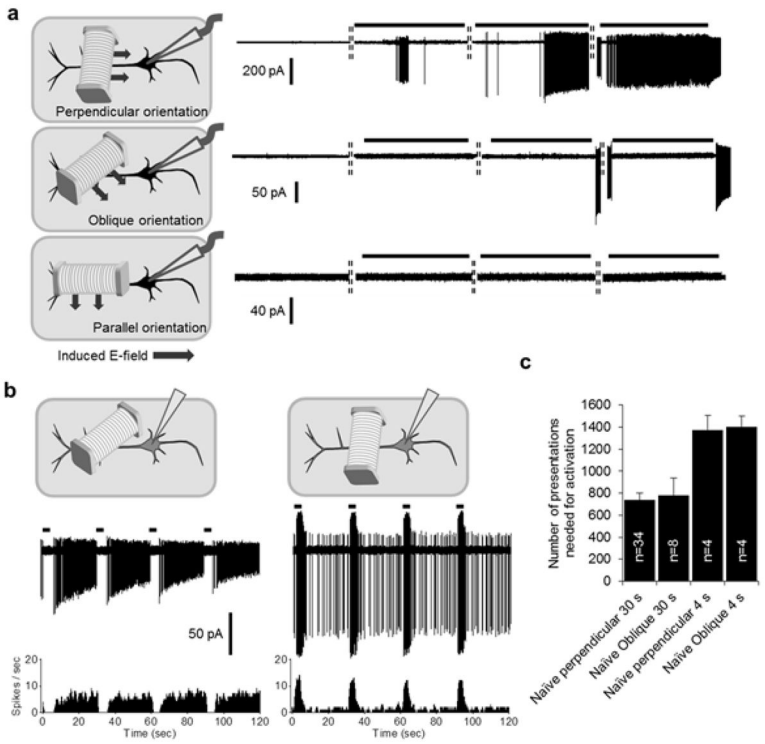

Fig. 5.

Coil orientation strongly influences responses. (a) (left) Schematic depicting three orientations of the coil relative to the long axis of the PN. (right) Typical response for each orientation. Black soma indicates a ‘naïve’ PN, i.e. one that had not been stimulated previously. Note the presence of ‘OFF’ responses to oblique orientations of the coil (middle). Horizontal bars represent the 30 s duration of the 10 Hz stimulus train. The dashed vertical lines between traces indicate 20 s intervals between consecutive periods of stimulation. (b) (top panels) Schematic illustration of oblique (left) and perpendicular (right) orientations; gray somas indicate PNs that had previously been activated. (middle and bottom panels) Raw recording and corresponding PSTH (binsize = 0.1 s), respectively, elicited by the 4 s, 10 Hz stimulus. (c) Numbers of presentations needed to elicit spikes in naïve PNs for different coil orientations. The stimulus was a repetitive 10 Hz, 30 s duration, 20 s interval for the two leftmost bars and 10 Hz, 4s duration, 26 s interval for the two right-most bars. Error bars indicate S.E. Research supported by the Veterans Administration - RR&D (1I01 RX001663), the Rappaport Foundation, and by the NIH (NEI R01-EY023651 and NINDS U01-NS099700).